Supplementary Table

Table S1. The expression correlation between predicted miRNAs and C6orf120 in LIHC.

Gene	miRNA	R-value	P-value
C6orf120	hsa-miR-135b-5p	-0.030	0.567
C6orf120	hsa-miR-1-3p	-0.146	0.005
C6orf120	hsa-miR-27a-3p	-0.049	0.347
C6orf120	hsa-miR-27b-3p	0.018	0.736
C6orf120	hsa-miR-106b-5p	0.038	0.471
C6orf120	hsa-miR-155-5p	0.131	0.012
C6orf120	hsa-miR-20a-5p	-0.018	0.735
C6orf120	hsa-miR-597-5p	0.073	0.165
C6orf120	hsa-miR-153-3p	0.064	0.225
C6orf120	hsa-miR-106a-5p	0.092	0.077
C6orf120	hsa-miR-128-3p	0.097	0.062
C6orf120	hsa-miR-519d-3p	0.075	0.151

Table S2. The expression correlation between predicted lncRNAs and hsa-miR-1-3p in LIHC.

miRNA	lncRNA	R-value	P-value
hsa-mir-1-3p	CCDC18-AS1	-0.078	0.130
hsa-mir-1-3p	LAMTOR5-AS1	-0.028	0.583
hsa-mir-1-3p	LINC00622	0.027	0.600
hsa-mir-1-3p	MIR29B2CHG	0.051	0.322
hsa-mir-1-3p	CYTOR	-0.028	0.591
hsa-mir-1-3p	MIR4435-2HG	-0.017	0.749
hsa-mir-1-3p	ACAP2-IT1	-0.086	0.098
hsa-mir-1-3p	STX18-AS1	0.038	0.461
hsa-mir-1-3p	MIR4453HG	-0.021	0.686
hsa-mir-1-3p	FAM198B-AS1	-0.030	0.560
hsa-mir-1-3p	LINC00242	0.012	0.818

hsa-mir-1-3p	LINC00174	-0.025	0.629
hsa-mir-1-3p	LINC-PINT	-0.165	0.001
hsa-mir-1-3p	OTUD6B-AS1	-0.081	0.117
hsa-mir-1-3p	RMRP	0.066	0.204
hsa-mir-1-3p	FAM225B	0.083	0.111
hsa-mir-1-3p	FAM225A	0.060	0.246
hsa-mir-1-3p	LINC00707	-0.025	0.628
hsa-mir-1-3p	LINC01518	0.018	0.729
hsa-mir-1-3p	NUTM2B-AS1	0.055	0.290
hsa-mir-1-3p	NUTM2A-AS1	0.047	0.362
hsa-mir-1-3p	DNMBP-AS1	0.054	0.297
hsa-mir-1-3p	RPARP-AS1	0.020	0.698
hsa-mir-1-3p	NEAT1	-0.061	0.242
hsa-mir-1-3p	MALAT1	-0.033	0.530
hsa-mir-1-3p	SENCR	-0.027	0.602
hsa-mir-1-3p	C1RL-AS1	-0.005	0.926
hsa-mir-1-3p	HOTAIR	-0.018	0.731
hsa-mir-1-3p	LINC00641	-0.023	0.656
hsa-mir-1-3p	DHRS4-AS1	0.007	0.888
hsa-mir-1-3p	VASH1-AS1	0.109	0.036
hsa-mir-1-3p	SNHG14	0.060	0.246
hsa-mir-1-3p	TMEM202-AS1	0.04	0.445
hsa-mir-1-3p	UBL7-AS1	0.062	0.231
hsa-mir-1-3p	LINC01197	0.008	0.873
hsa-mir-1-3p	COX10-AS1	0.024	0.644
hsa-mir-1-3p	MAPT-IT1	-0.057	0.275
hsa-mir-1-3p	SOX9-AS1	0.082	0.112
hsa-mir-1-3p	LINC00482	0.031	0.546
hsa-mir-1-3p	UCA1	0.056	0.281
hsa-mir-1-3p	SDCBP2-AS1	-0.046	0.376
hsa-mir-1-3p	LINC00261	-0.002	0.964
hsa-mir-1-3p	SMIM25	-0.043	0.403
hsa-mir-1-3p	MIAT	-0.041	0.424

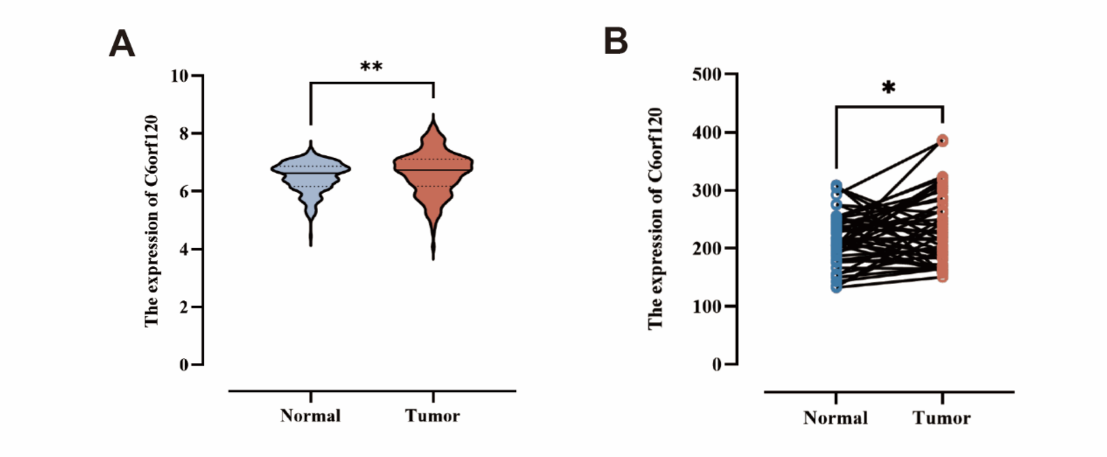

Figure S1. The expression of C6orf120 in LIHC. (A) Comparison of the expression of C6orf120 in cancer and normal from GSE14520. (B) Comparison of the expression of C6orf120 in cancer and paracancerous from GSE76427.

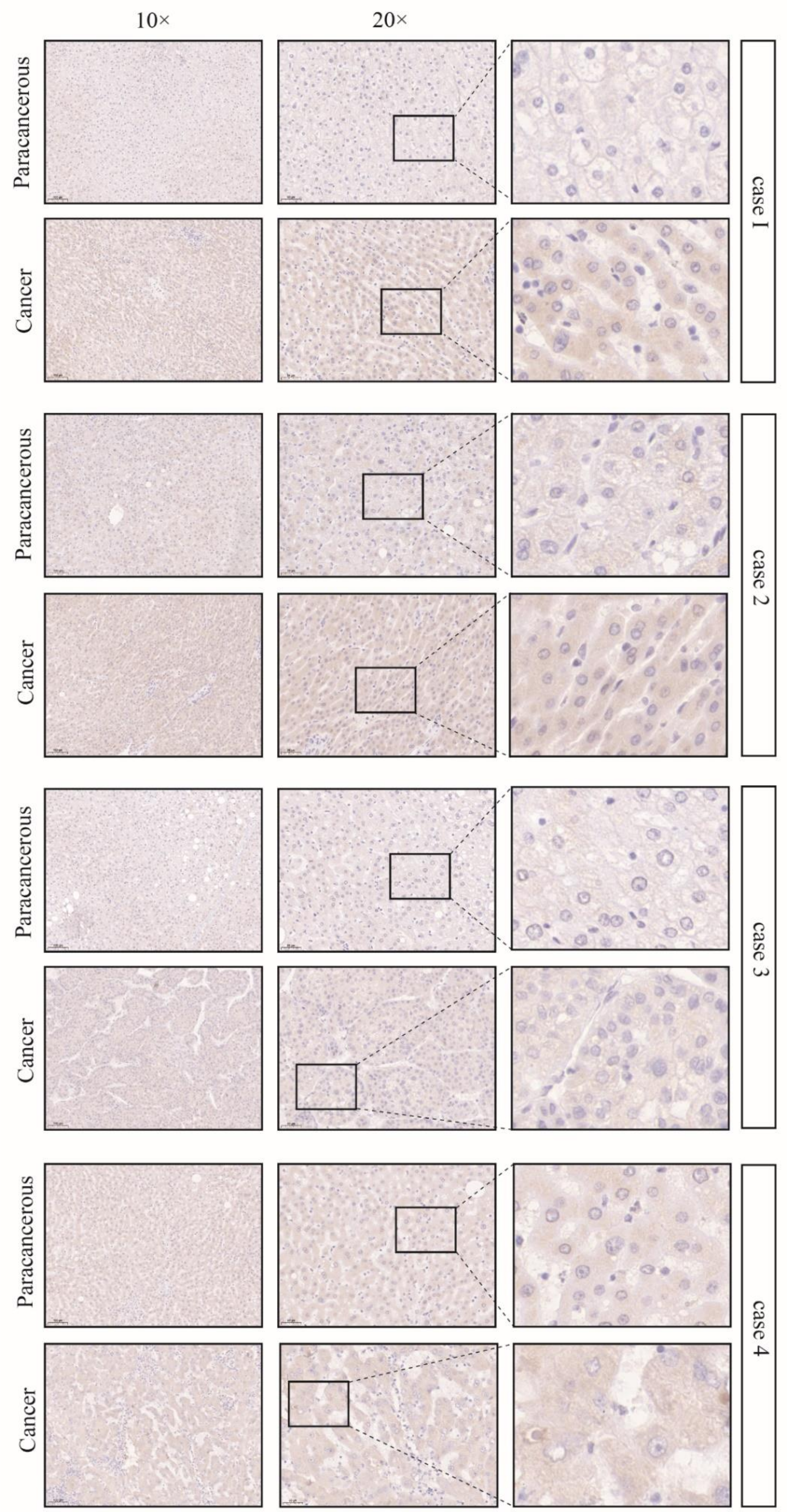

Figure S2. The expression of C6orf120 in LIHC was detected by immunohistochemical.

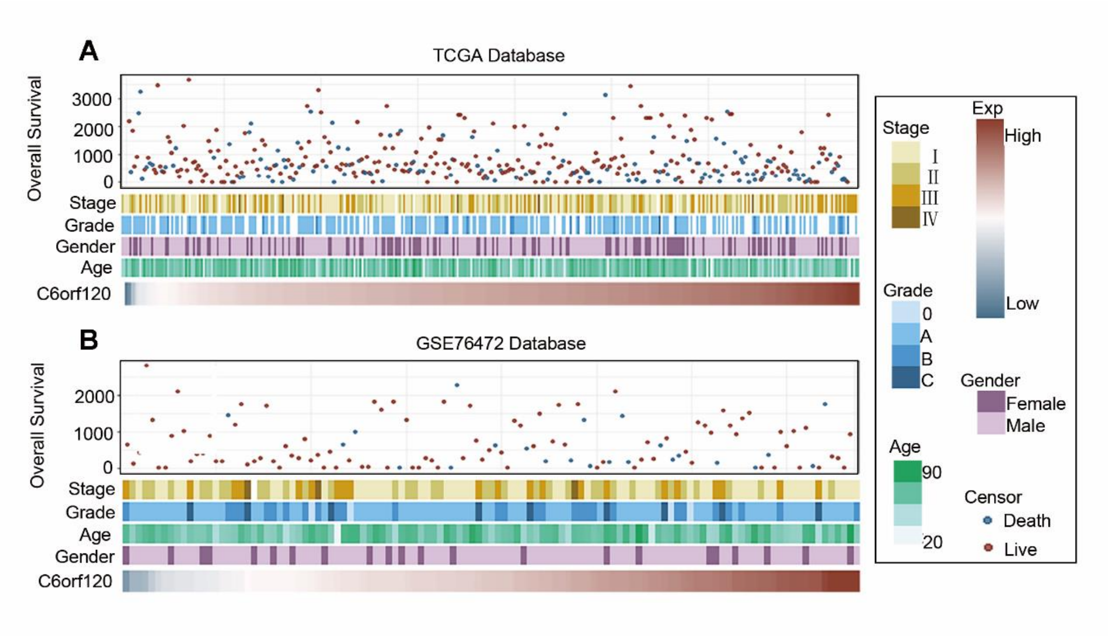

Figure S3. Association between C6orf120 and clinicopathological characteristics of LIHC. (A) Heatmap of the association between the expression level of C6orf120 and clinicopathological features in the TCGA database. (B) Heatmap of the association between the expression level of C6orf120 and clinicopathological features in the GSE76472 database.

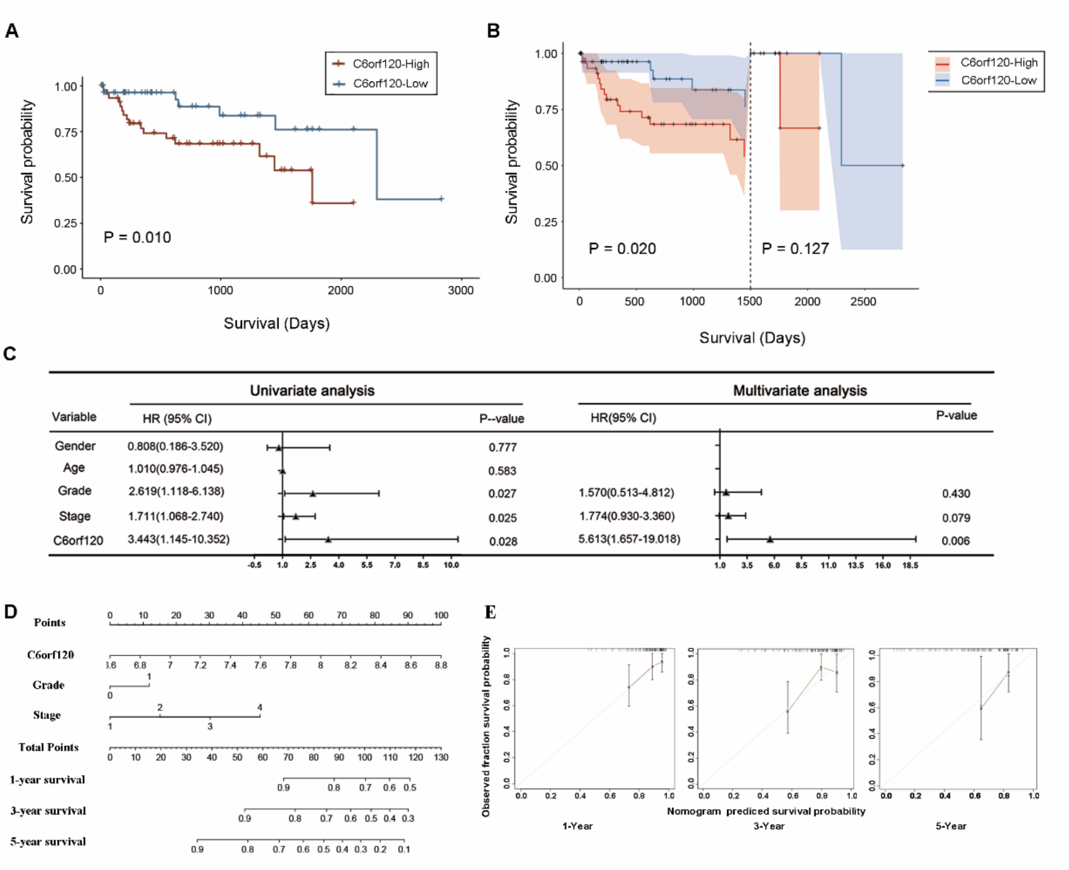

	Univariate analysis		Multivariate analysis	
Variable	HR (95% CI)	P--value	HR(95% CI)	P-value
Gender	0.808(0.186-3.520)	0.777		
Age	1.010(0.976-1.045)	0.583		
Grade	2.619(1.118-6.138)	0.027	1.570(0.513-4.812)	0.430
Stage	1.711(1.068-2.740)	0.025	1.774(0.930-3.360)	0.079
C6orf120	3.443(1.145-10.352)	0.028	5.613(1.657-19.018)	0.006

Figure S4. High expression of C6orf120 indicated poor survival in patients with LIHC. (A) Kaplan-Meier survival curve showing a comparison of OS between patients with LIHC presenting high and low C6orf120 expression in the GSE76427 cohort, and (B) landmark analyses（0 to 5 years）are shown. (C) Forest map showing univariate and multivariate analysis about overall survival (OS) of LIHC patients in the GSE76427 database. (D) For patients with LIHC in the GSE76427 database. A nomogram based on grade, stage and C6orf120 was constructed to estimate the probability of 1-, 3-, and 5-year OS. (E) Nomogram calibration plots for determining the probability of 1-, 3-, and 5-year survival.

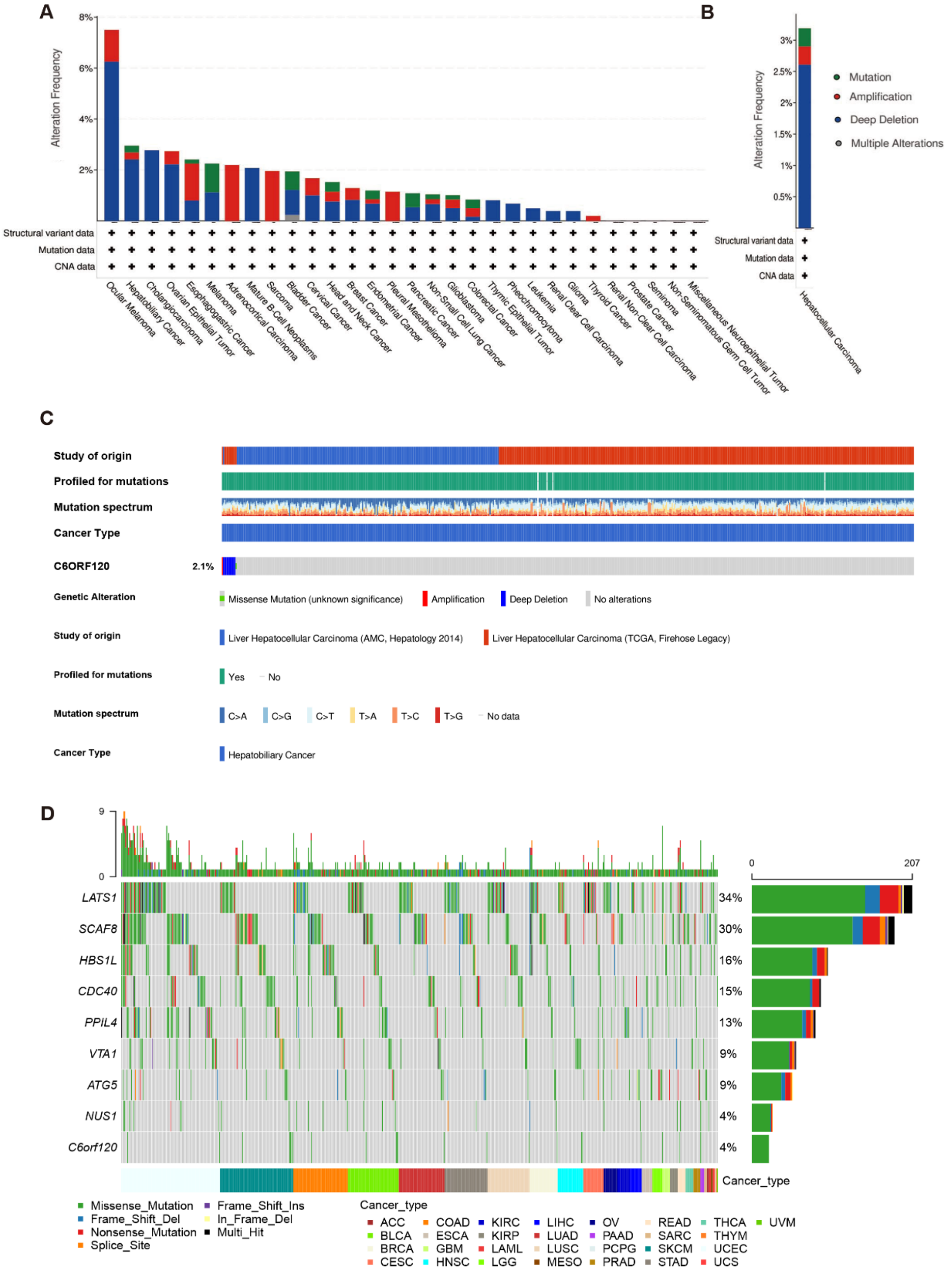

Figure S5. Mutation Landscape of C6orf120. cBioPortal was used to display the types of C6orf120 mutation in (A) pan-cancer and (B) LIHC. (C) OncoPrint visual summary of the alterations in the C6orf120 gene from the cBioPortal database. (D) Waterfall maps provide the situation of the SNV of the C6orf120-related genes set in the pan-cancer.

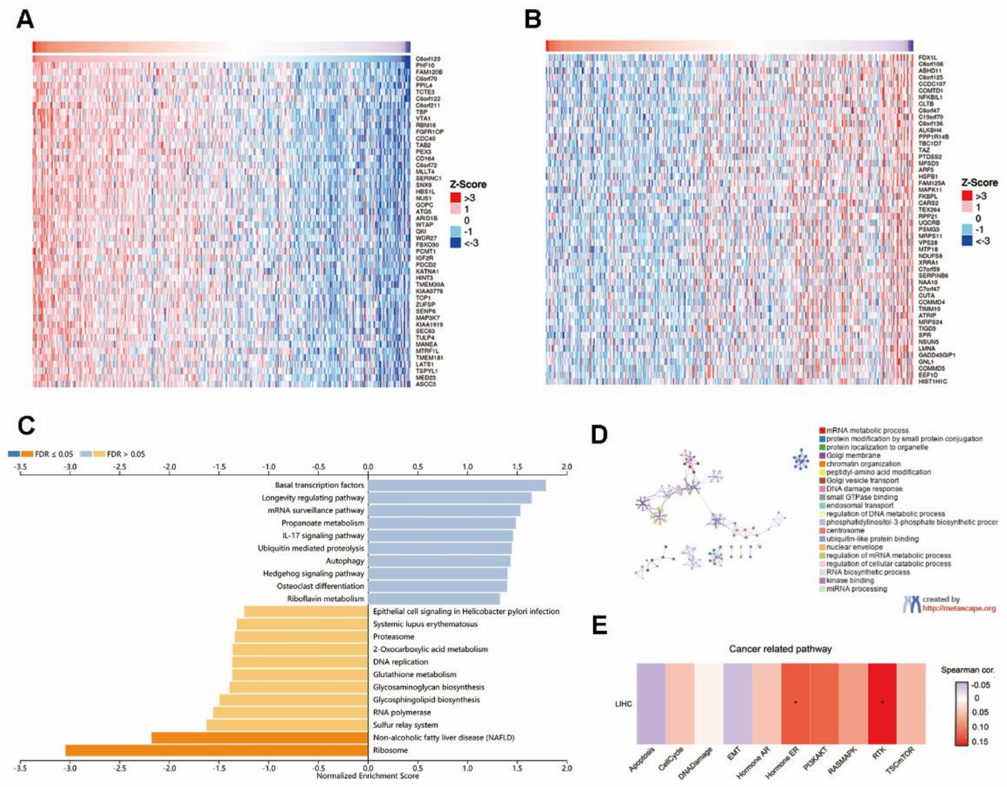

Figure S6. Related genes and functional enrichment analysis of C6orf120 in LIHC. (A, B) The top 50 positive coexpression genes and negative coexpression genes of C6orf120 in the heatmap in LIHC were analyzed by the LinkedOmics database. (C) GSEA analysis of C6orf120 by the LinkedOmics database. (D) Network of GO-enriched terms colored by cluster ID, where nodes that share the same cluster ID are typically close to each other. € GSVA analysis of C6orf120 and cancer-related pathways by GSCA tool.

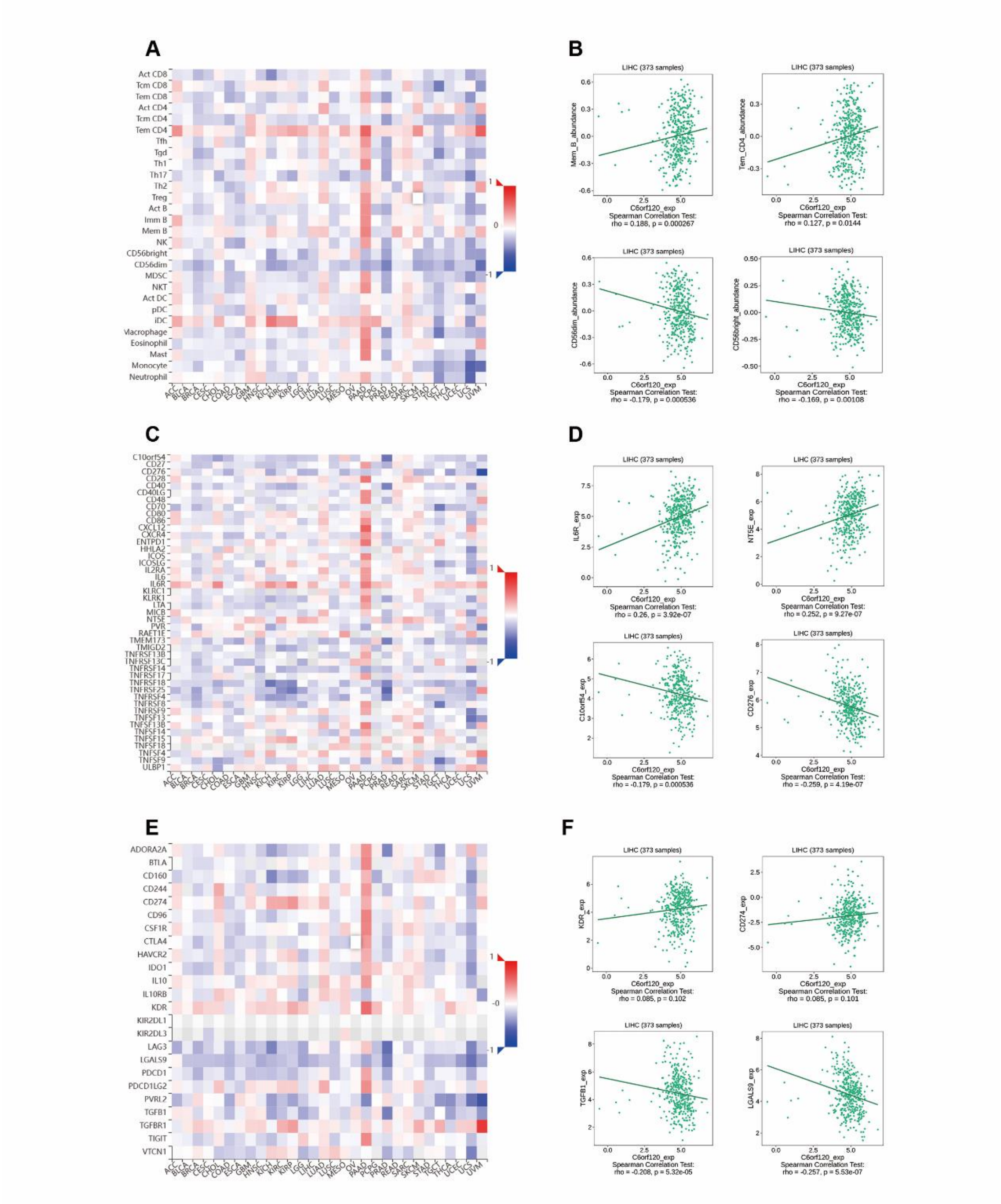

Figure S7. Correlation analysis of C6orf120 level and immunity. (A) Relations with tumor-infiltrating lymphocytes in pan-cancer. (B) The top two positive correlation results and the top two negative correlations in tumor-infiltrating lymphocytes. (C) Relations with immune stimulators in pan-cancer. (D) The top two positive correlation results and the top two negative correlations in immune stimulators. (E) Relations with immune inhibitors in pan-cancer. (F) The top two positive correlation results and the top two negative correlations in immune inhibitors (red is positively correlated and blue is negatively correlated; rho > 0 indicates positive, and rho < 0 indicates negative).

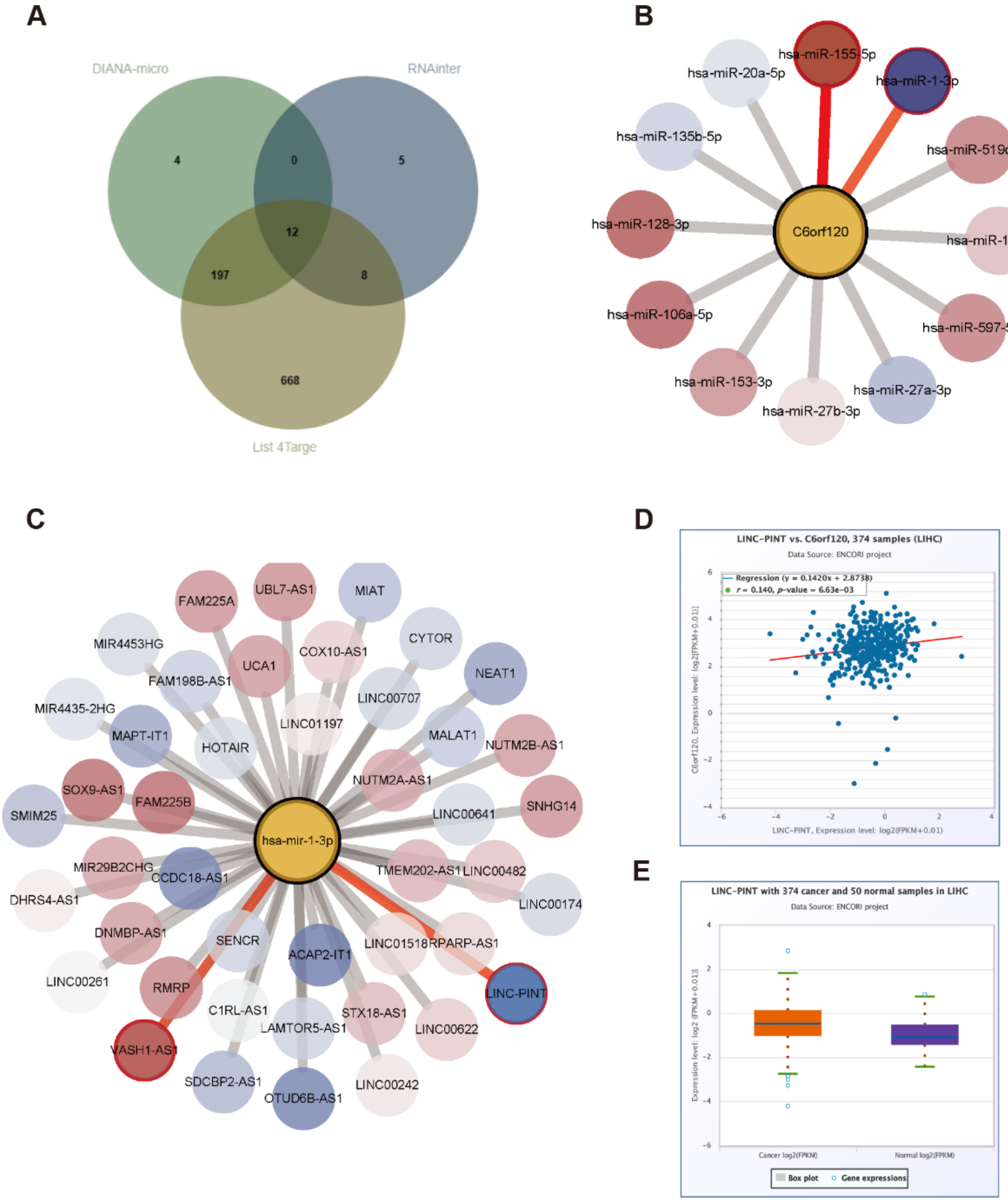

Figure S8. Prediction of the C6orf120-related ceRNA regulatory network in LIHC. (A) Venn diagram showing the results of the predicted target microRNAs (miRNAs) for C6orf120, as identified by the TargetScan, DIANA-microT, and RNAinter databases. (B) The miRNA-C6orf120 regulatory network. (C) The ceRNA-mRNA regulatory network. (D) The correlation between the expression levels of C6orf120 and LINC-PINT. (E) The expression of LINC-PINT in LIHC and compared to normal control samples.